REPORT DOCUMENTATION PAGE

Form Approved
OMB No. 0704-0188

1. Agency Use Only *(Leave blank).*	2. Report Date.	3. Report Type and Dates Covered.
	1989	Proceedings

4. Title and Subtitle.
Use of Polarization methods in earth resources investigations

5. Funding Numbers.
Program Element No. 61153N
Project No.
Task No.
Accession No. DN250010

6. Author(s).
M. J. Duggin, S. A. Israel, V. S. Whitehead, J. S. Myers, and D. R. Robertson

7. Performing Organization Name(s) and Address(es).
Naval Oceanographic and Atmospheric Research Laboratory*
Stennis Space Center, MS 39529-5004

8. Performing Organization Report Number.
PR 089:057:321

9. Sponsoring/Monitoring Agency Name(s) and Address(es).
Office of the Chief of Naval Research
Arlington, VA 22217-5000

10. Sponsoring/Monitoring Agency Report Number.
PR 089:057:321

11. Supplementary Notes.
*Formerly Naval Ocean Research and Development Activity
**Continued on next page

12a. Distribution/Availability Statement.
Approved for public release; distribution is unlimited.

12b. Distribution Code.

13. Abstract *(Maximum 200 words).*
Relatively little attention has been paid to the potential of polarization techniques to provide additional information for the mapping of earth resources, compared to the published work concerning other active and passive remote sensing systems. Recently, a substantial number of polarized light images of a variety of terrestrial scenes have been obtained from the Space Shuttle. A boresighted pair of Hasselblad cameras was used, in which polarization filters were fitted. The polarization directions were perpendicular to each other for the two cameras. Image pairs were acquired with one image being of maximum intensity, and the other showing minimum intensity. Selected pairs of images, obtained using black and white films, were digitized. The images were registered and compared, using digital image analysis techniques. Differences due to polarization were observed, these included intensity and contrast differences, together with differences in the spatial frequency, orientation and population of observable contrast boundaries. It was found empirically that some digital image analysis techniques enhanced the differences. A comparison of the**

14. Subject Terms.	15. Number of Pages.
(U) Anti-submarine Warfare; (U) Detectors; (U) Oceanography	12
	16. Price Code.

17. Security Classification of Report.	18. Security Classification of This Page.	19. Security Classification of Abstract.	20. Limitation of Abstract.
Unclassified	Unclassified	Unclassified	SAR

**enhanced difference images, obtained from the polarization pairs, with the intensity data that would have been obtained without the aid of polarization filters, confirms that a considerable degree of new, useful information may be obtained by the use of polarization techniques. This new information was most helpful in better defining the observed ground features in the cases studied. This is because the better definition of contrast boundaries, improvement of contrast across boundaries, improvement of shadow detail and reduction of noise level increases the useful information in an image, and improves its interpretability.

PROCEEDINGS REPRINT

SPIE—The International Society for Optical Engineering

Reprinted from

Polarization Considerations for Optical Systems II

9-11 August 1989
San Diego, California

Volume 1166

Box 10, Bellingham, Washington 98227 USA. Telephone 206/676-3290.

Invited Paper

Use of polarization methods in earth resources investigations

M. J. Duggin*, **, S. A. Israel*, V. S. Whitehead+, J. S. Myers++, D. R. Robertson+

*308 Bray Hall, CESF, State University of New York, Syracuse, NY 13210
+Code SN15, NASA-Johnson Space Center, Houston, TX 77058
++M/S 240-12 Aircraft Data Facility, NASA Ames Research Center, Moffett Field, CA 94035
**Also Summer Faculty at Naval Ocean Research and Development Activity, Code 321,
Stennis Space Center, MS 39529-5004

ABSTRACT

Relatively little attention has been paid to the potential of polarization techniques to provide additional information for the mapping of earth resources, compared to the published work concerning other active and passive remote sensing systems. Recently, a substantial number of polarized light images of a variety of terrestrial scenes have been obtained from the Space Shuttle. A boresighted pair of Hasselblad cameras was used, in which polarization filters were fitted. The polarization directions were perpendicular to each other for the two cameras. Image pairs were acquired with one image being of maximum intensity, and the other showing minimum intensity. Selected pairs of images, obtained using black and white films, were digitized. The images were registered and compared, using digital image analysis techniques. Differences due to polarization were observed, these included intensity and contrast differences, together with differences in the spatial frequency, orientation and population of observable contrast boundaries. It was found empirically that some digital image analysis techniques enhanced the differences. A comparison of the enhanced difference images, obtained from the polarization pairs, with the intensity data that would have been obtained without the aid of polarization filters, confirms that a considerable degree of new, useful information may be obtained by the use of polarization techniques. This new information was most helpful in better defining the observed ground features in the cases studied. This is because the better definition of contrast boundaries, improvement of contrast across boundaries, improvement of shadow detail and reduction of noise level increases the useful information in an image, and improves its interpretability.

1. INTRODUCTION

Although many laboratory studies of polarization have been made compared to research studies in the unpolarized visible and infrared regions there has been little activity to attempt to translate polarization phenomena into a technique for remotely mapping earth resources or to study meteorological or oceanographic phenomena. Egan[1] deduced from laboratory measurements on vegetation that information gained from polarization measurements could assist in the mapping of agricultural crops. Vanderbilt, Grant and Daughtry[2], Egan[3], Slater[4], and Talmadge and Curran[5] point out the potential value of polarization techniques in remote sensing. Coulson[6] and Coulson, Bouricius and Gray[7] have made ground and laboratory measurements of the view angle and illumination angle dependence of the polarization of light reflected from surfaces. More recent measurements have been made by Vanderbilt, Grant and Daughtry[2]. Halajian and Hallock[8] have investigated polarimetric mapping as a remote sensing tool. Curran[9] has reported on the use of aerial polarimetric photographic methods in soil moisture investigations.

More recently, the advent of space shuttle has enabled the exploratory use of polarized light photography of the earth for the preliminary assessment of the utility of polarization methods for earth resources mapping, as reported by Coulson, Whitehead and Campbell[10]. A recent book by Coulson[11] provides a thorough coverage of present knowledge regarding polarization effects of the atmosphere.

In this paper, we report upon further preliminary investigations of polarized light photography of the earth for earth resources, meteorological and oceanographic observation. Due to the constraints of time and space, only part of our investigations are reported here.

2. DISCUSSION OF PAST WORK

The mean polarization state of radiance reflected from a given feature may change with time, due to the change with time in the orientation of the mean electric vector. The polarized wave is the resultant of the interaction of the ensemble of waves propagated in the same direction but with different phase and amplitude at different orientations about the direction of propagation. In the case of linear polarization, the orientation of the plane of the resulting polarized wave about the direction of propagation does not vary with time. In the case of circular polarization, the ensemble of propagated waves produces the same effect as two orthogonal waves of equal amplitude which are out of phase by a constant phase angle. The resulting wave is of constant amplitude but the plane of the electric vector rotates with time about the direction of propagation. In the case of elliptical polarization, the amplitude of the resultant wave varies with time as the plane of the resultant wave rotates about the direction of propagation. These three states are shown in Fig. 1. Here, we are looking down the axis of propagation at the locus traced out by the amplitude of the resultant electric wave. The orientation of the semimajor ellipse of the polarization vector will depend upon the magnitude and polarity of the two components of the resultant electric field vectors into which the ensemble of waves propagating in the same direction can be decomposed.

In order to define the state of polarization, we must consider those properties that we need to measure that will characterize its polarization. G. G. Stokes, in 1852, introduced four quantities that are functions only of the observables of the electromagnetic wave and are known as Stokes parameters. A useful description is in Hecht[12] and in Egan[3].

Egan[3] gives a definition of the four Stokes parameters in terms of the amplitudes of the electromagnetic waves in the x and y directions which are mutually orthogonal, with x being in the plane of the electric vector for minimum polarization and y being in the plane of the electric vector for maximum polarization, which corresponds to the directions of maximum and minimum intensity, respectively, as an analyzer is rotated in the beam.

$$I = \langle A_x^2 + A_y^2 \rangle = A^2 \tag{1}$$

$$Q = \langle A_x^2 - A_y^2 \rangle \tag{2}$$

$$U = \langle 2 A_x A_y \cos \gamma \rangle \tag{3}$$

$$V = \langle 2 A_x A_y \sin \gamma \rangle \tag{4}$$

This is a time average of the definition given by Chandrasekhar[13]. Here, $\langle \quad \rangle$ indicates time averaging. A_x and A_y are the magnitudes of the representative average electromagnetic waves in the x and y directions, A^2 is intensity and γ is the phase angle between A_x and A_y. The radiant intensity I is related to the other three Stokes parameters by the equation

$$I^2 = Q^2 + U^2 + V^2 . \tag{5}$$

Q is the difference in radiant intensity between the mutually orthogonal x and y directions used to specify A_x and A_y. In the case where the x and y directions represent the directions of the electric vector for maximum and minimum intensity, respectively, then

$$Q = I_{max} - I_{min} , \tag{6}$$

whereas, for this case

$$I = I_{max} + I_{min} . \tag{7}$$

In the case of partially polarized, linear, quasimonochromatic light, if we rotate an analyzer in the beam, then there will be an orientation at which the transmitted irradiance is a maximum. This will be at right angles to the orientation where it is at a minimum. In this case, the maximum intensity will consist of the sum of the polarized (I_p) and unpolarized (I_u) components, while the minimum component will consist only of the unpolarized component I_u.

$$\text{Thus } Q = (I_p + I_u) - (I_u) \tag{8}$$

$$= I_{max} - I_{min} , \tag{9}$$

whereas

$$I = I_{max} + I_{min} = I_p + 2I_u . \tag{10}$$

Then the degree of polarization (P) of the beam is given by

$$P(^{\circ}_{0}) = 100\, x\, \frac{<A_x^2 - A_y^2>}{<A_x^2 + A_y^2>} = 100\, \frac{Q}{I} = 100\, x\, \frac{I_{max} - I_{min}}{I_{max} + I_{min}} . \tag{11}$$

The shape of the polarization ellipse is given by

$$\varkappa = \tan^{-1} \frac{b}{a} , \tag{12}$$

where a and b are the semimajor and the semiminor axes respectively. Also

$$\varkappa = \frac{1}{2} \tan^{-1} \frac{V}{(Q^2 + U^2)^{1/2}} . \tag{13}$$

Whether the polarization is right-handed or left-handed depends upon the sign of V. The orientation of the polarization ellipse with respect to a reference direction is given by

$$\xi = \frac{1}{2} \tan^{-1} \left(\frac{U}{Q} \right) . \tag{14}$$

Methods have been summarized by Talmadge and Curran[5] for measuring reflected, polarized light with linear polarizing filters set at different orientations to determine the Stokes parameters. As observed by Coulson, Whitehead and Campbell[10] and by Talmadge and Curran[5], the Stokes parameter V is generally very small after reflection from the earth's surface. V represents the amount of circularly polarized light (e.g., Egan[3]). Indeed, Spohr[14] reports that the contribution of the circular polarized component to the total intensity is two orders of magnitude less than the contribution of the linear polarized component. Since V is very small, Prosh, Hennings and Raschke[15] determine the Stokes parameters I, Q, and U from radiance measurements using polarizers in front of separate radiometers. They compute the components of the Stokes vector, where the polarization filters are at respective orientations about the optic axis of the detectors of 0°, 60° and 120°. The Stokes vector components, expressed in terms of the transmitted radiance $\bar{I}_0$, $\bar{I}_{60}$, $\bar{I}_{120}$ are

$$I = \frac{2}{3} \left(\bar{I}_0 + \bar{I}_{60} + \bar{I}_{120} \right) \tag{15}$$

$$Q = \frac{2}{3} \left(2\bar{I}_0 - \bar{I}_{60} - \bar{I}_{120} \right) \tag{16}$$

$$U = -\frac{2}{\sqrt{3}} \left(\bar{I}_{120} - \bar{I}_{60} \right) \tag{17}$$

Prosh, Hennings and Rashke converted the output voltages from the three-detector video polarimeter to color coordinates for display using a color video monitor. The azimuth of polarization ($\varkappa$) defines tint, and the degree of polarization (P) defines hue. They reported that their instrument and technique provided useful quick-look data and, when used on an airborne platform, enhanced the discriminability of features on the ground. Walraven[16] used a 35mm camera to obtain sets of four slides of scenes using a polarizing filter at 0°, 45°, 90°, and 135° relative

orientation of the polarization direction about the optic axis of the camera. The intensity of the radiation that passes through the polarization filter is given by

$$I'(\theta) = 1/2(I + Q\cos 2\theta + U\sin 2\theta) , \tag{18}$$

where θ is the angle of the transmission axis of the polarizer about the optic axis of the camera, with respect to the horizontal. If measurements are successively made with $\theta = 0°, 45°, 90°$, and $135°$, then the resulting intensity is

$$I'(0) = 1/2(I + Q) , \tag{19}$$

$$I'(45) = 1/2(I + U) , \tag{20}$$

$$I'(90) = 1/2(I - Q) , \tag{21}$$

$$I'(135) = 1/2(I - U) . \tag{22}$$

From these equations, Walraven deduced the Stokes parameters:

$$I = 1/2[I'(0) + I'(45) + I'(90) + I'(135)] \tag{23}$$

$$Q = I'(0) - I'(90) \tag{24}$$

$$U = I'(45) - I'(135) \tag{25}$$

With the polarizer set at each of the four angles defined above, the four photographic images were obtained with the same f-stop. They were then digitized and registered. Images of I, P, ζ were obtained:

$$P = \frac{1}{I}(Q^2 + U^2)^{1/2} \tag{26}$$

The Stokes parameter V is very small, and the azimuth of polarization with respect to the horizontal (ζ) is given by equation (14).

Walraven showed images of I, (1-P) and ζ for four natural scenes. He used (1-P) instead of the degree of polarization P, since the degree of polarization appears to be inversely proportional to the albedo. He showed that the polarization images provided new and useful information about a scene beyond that available from an intensity image.

As Walraven[16] points out, the measurements made in the laboratory are considerably more complicated when made in the field. Illumination is no longer from a point source, but partly from scattered, diffuse sky illumination which is polarized to an extent which depends on the angular location of each elemental source of irradiance in the sky. The irradiance from the sun is unpolarized, although that from the sky is polarized to an extent which depends on sun angle and upon the reflectance of terrain, as shown by Coulson.[11,17] Variations in composition, heterogeneity and topography may also arise at both a resolvable and at a subresolution level (e.g., Duggin[18]). Walraven also points out that since man-made surfaces are unusually smooth, they exhibit higher than usual polarization. Darker surfaces tend to exhibit larger polarizations because the single scattering component is larger than that for light surfaces, where multiple scattering prevails.[16]

Coulson, Whitehead and Campbell[10] have observed that there is little information regarding orbital observations of polarization of light reflected from the earth's surface, although there is some data on the reflection of polarized light from the earth's atmosphere.[19] Coulson, Whitehead and Campbell[10] studied polarization measured from digitized, registered polarization photographic pairs obtained from space shuttle flight STS-51. These authors analyzed image data obtained from a synchronized hand-held camera pair in which both cameras were attached to a common frame and bore-sighted. The linear polarization filters had polarization axes oriented at right angles to each other about the optic axis. The cameras were pointed at terrestrial targets and rotated about the optic axis until one camera

showed maximum intensity, and the other showed minimum intensity through the viewfinders: such judgments were empirical. The photographs were subsequently digitized and analyzed to provide polarization images. The authors concluded that there was potential for the application of polarization photography from orbit in studies of the earth. They observed degrees of polarization of up to 0.5. The degree of polarization varied systematically across the image. It was reported that the polarization image made some patterns discernable which were not discernible on the intensity images. Further, it was reported that the use of polarization improved the signal-to-noise ratio.

In this paper, we report an analysis of the black-and-white film image pairs from space shuttle mission STS-51A.

Since image pairs, representing maximum and minimum intensity only, were obtained, it is not possible to calculate all of the Stokes parameters. If we assume, on the basis of prior work[10,14,15] that the circular component of polarization of radiance reflected from the earth is close to zero, then we could obtain more complete information if we have sequences of three images with the polarization filter oriented at three angular positions about the optical axis of the camera system. In addition to the polarization filters whose polarization directions are orthogonal, an additional channel with the polarization filter oriented at (say) 45° to the maximum could be used.

However, the data analyzed were collected for exploratory purposes. The analyses of this two-channel data clearly show that as found by Coulson, Whitehead and Campbell[10] there is ample reason to expect a great deal of benefit for earth resources investigations from the orbital acquisition and analysis of polarized light imagery for analysis in conjunction with earth resources studies.

3. EXPERIMENTAL DATA

The polarization image pairs were obtained on space shuttle mission STS-51A (October 1984). Photography was obtained using a boresighted pair of Hasselblad cameras, which were synchronized to produce simultaneous exposures. Polarization filters were fitted to both cameras, and the directions of polarization were orthogonal to each other about the optic axis of the camera system. The camera pair was rotated about its optic axis by the astronaut photographer so that when a target of interest was selected, the image through one viewfinder was of maximum brightness, and the image through the other viewfinder was of minimum brightness. Thus, two images were obtained: one of maximum intensity and the other of minimum intensity. We used second-generation film that was processed to positive transparency. There is no way of knowing the precision in selecting the maximum and minimum intensity, nor of knowing the change in polarization caused by the space shuttle windows. Therefore, the selection of angles was assumed to be exactly correct, and the potential impact of the space shuttle windows on polarization was ignored. The images were digitized using a Diconix digitizer and VAX 11/780 computer system at NASA's Johnson Space Center. Unfortunately, the film had no sensitometry strip; thus the films from both cameras were assumed to be identically processed, so that the calibration of focal plane irradiance to photographic density would be the same in each case. Following this assumption, the degree of polarization could be obtained from digitized, registered, image pairs. We used 8-bit quantization during image digitization and registered the images. The digitized, registered, image pairs were than manipulated using standard image analysis techniques as described in the following section.

4. ANALYSIS AND RESULTS

We selected 20 images from the black and white image pairs obtained on Space Shuttle Mission STS-51A for further study. The digitized images were registered using nearest neighbor interpolation, so the radiometry of the images would not be modified. While the different images obtained different radiometric information, it was considered that spatial information in the form of contrast boundaries and texture would be different in the two images. While only the degree of polarization (i.e., the first two Stokes parameters) may be obtained from an image pair, information on contrast boundaries and on texture differences between components of the image pair should be able to be extracted, given the appropriate analysis. To this end, after carefully digitizing the image pairs using the ICONIX facility at NASA Johnson Space Center, we performed digital image analysis on the IDIMS installation at NASA Ames Research Center; on the ERDAS installation at State University of New York ESF, Syracuse; and on the I²S System 600 at the Naval Ocean Research and Development Activity, Stennis Space Center, Mississippi.

Each image pair was scaled and individually displayed together with images of the sum and the difference; the ratio and difference divided by the sum. In an empirical investigation, we also combined the individual images, the sum, difference, and ratio, and difference divided by the sum images to provide input to a principal component analysis. Of course, the input images were strongly correlated, but the principal component images did, in some cases, provide a useful data enhancement. We also obtained beneficial pictorial image information by performing a principal components analysis, performing histogram equalization on the principal components images, and then applying the inverse transformation matrix. The results we obtained are extremely valuable, but we cannot completely explain at this time why such analyses are so effective.

Further work consisted of calculating the Fourier spectra of each of the images and of calculating the difference in Fourier spectra between the components of the image pair. The difference in Fourier spectra will show the difference in both contrast boundaries and edge features provided by contrast differences between the two images. A significant azimuthal anisotropy was observed to occur in the spatial frequency plane. The appearance of this property was not altogether surprising, since differences in the shadow components between the polarization image pair will occur due to the polarization characteristics of the ground and the polarization characteristics of the atmosphere, and will be strongly affected by sun-target-sensor geometry. Shadowed areas will be almost entirely diffusely illuminated, so that differences in the depth of shadow will be recorded as difference in the degree of polarization. Indeed, one objective of our investigation is to determine whether and to what extent polarized light may be used to enhance detail in shadowed areas. Thus, the spatial frequency information contained in each image of the polarization pair will be impacted by the topography and optical characteristics of the ground, and by atmospheric conditions, as well as by view and illumination geometry. Further, water bodies will strongly polarize reflected light; the degree of polarization will depend upon the azimuth angle between the planes containing the detected ray and the corresponding radiance from the sun. Appropriate selection of illumination and imaging conditions may therefore reasonably be expected to yield useful hydrological information. Oblique views of anisotropic ground scenes, illuminated from the side will generally result in a greater degree of difference between the Fourier spectra of polarization image pairs.

An example of an image obtained over a land area containing hydrologic features (Niger River in Mali) is shown in Fig. 2. The components of the polarization pair, images A and B, the difference image (A-B), the sum image (A + B), the ratio image (A/B) and the degree of polarization image (A-B)/(A + B) are shown. The Niger River is displayed well in Fig. 2a, but is almost invisible in Fig. 2b, the other component of the polarization pair. The difference image (Fig. 2c) provides slight enhancement of the river system, but while the sum image (Fig. 2d) is better than image B, it has less hydrological information than does image A, as one might expect. The degree of polarization image (Fig. 2e) does not enhance the river system, but does enhance sand dune structure. The ratio image (Fig. 2f) does not provide more information on the river than the degree of polarization image.

A principal component analysis was performed with input consisting of the individual images, the sum, difference, the ratio, and polarization images. The first and second principal components images are shown in Figs. 2(g) and 2(h). Clearly, much more complete information on the Niger River and its tributaries is contained in the second principal component image than in any of the input images (Figs. 2(a)-2(f)). A further procedure was also investigated, since the input images were highly correlated. The principal components were histogram-equalized, and the inverse transformation matrix was applied. The resulting first inverse transform image (essentially an enhanced version of image A, containing information from all of the other input bands) is shown in Fig. 2(i). It is not clear why additional information was obtained from this treatment of the strongly correlated input images. However, we present this empirical data as evidence that digital image analysis can provide a means of extracting maximum information from the differences between the input polarization image pair. We then present this information in a single image that will facilitate mapping a specific feature of interest.

We also explored the differences in the spatial frequency spectra of features delineated by contract boundaries in the two images. The maximum and minimum intensity images, which correspond to the minimum and maximum polarization, respectively, contain contrast and contrast boundary information that is different in each image. The delineation and recognition of features will depend largely on the recognition of contrast boundaries. If the

intensity information differs from one image to another, then the contrast boundary information will differ between the images. Once the contrast across a boundary falls below a certain level, the boundary may not be detected. The subtraction of the Fourier spectrum of one image from that of the other image constituting the polarization pair will show the difference in the spatial frequencies at which contrast boundaries occur in the image pair, and will show the azimuthal distribution with which they occur. The frequency of occurrence of boundaries appearing with given spatial frequencies at given azimuthal orientations will be shown by the intensity of points represented in the frequency plane. The difference in the Fourier transforms of the two images is shown in Fig. 2(j). Clearly, there is not only a difference in the frequency of occurrence in contrast boundaries between the images, but there is also an azimuthal anisotropy. One might expect this event, since the features on the images do, by inspection, have a clear, preferred, azimuthal orientation.

A key point to remember is that the unpolarized images would be similar to the sum image (A + B) shown in Fig. 2(d). Here, the details of the river and its tributaries and lakes are far less evident than is the case in the original image A (Fig. 2(a)), the difference images (A-B) shown in Fig. 2(c) or the second principal component image shown in Fig. 2(h). The first inverse principal component image shown in Fig. 2(i) is probably the most useful image for the delineation of river features. Therefore, the use of polarization characteristics as a channel of information is most helpful in revealing new information.

While the above example deals with hydrological information, a geological example is shown in Fig. 3. The El Richat structure in Mauritania has been the subject of some discussion. It is uncertain whether this feature is the result of the impact of a large meteor, as is the case for Diablo Canyon. Differences in intensity and in contrast across boundaries are clear from careful comparison of the maximum and minimum polarization images shown in Figs. 3(a) and 3(b), which constitute the polarization pair. The differences are clearer from reference to the difference image (A-B), which is shown in Fig. 3(c), and clearer still from reference to the normalized difference (i.e., polarization) image (A-B)/(A + B), which is shown in Fig. 3(d). These images have been digitally enhanced, and fine detail is present in the polarization image, which was not present in either components of the original image pair. The sum image (A + B) is shown in Fig. 3(e) and is close to what might be obtained by conventional (i.e., nonpolarized) photography. Comparison of the sum image with the difference image, the polarization (normalized difference) image and the ratio image shown in Fig. 3(f) clearly demonstrates that the recording of polarization information yields new information. In particular, the relief topography is much more evident in the difference, the ratio and the polarization images than is the case in the sum image. Since the illumination of shadowed areas is almost entirely by diffuse irradiance, which is polarized, it is not surprising that the upwelling radiance from shadowed areas is strongly polarized, the degree of polarization depending upon the depth of shadow. We have had some positive indications that additional information in shadowed areas may be obtained by the digital analysis of polarized image pairs obtained over shadowed regions. However, more experimental study is needed before it may be determined fully whether and what extent this is so.

5. CONCLUSIONS

In this study, we have shown only a representative analysis performed on two pairs of images. The polarized image pairs discussed were obtained over terrestrial targets of hydrological and geological interest. We found that the differences between the image pairs contained a significant amount of information on contrast, contrast boundaries, shadow, and such terrestrial features as rivers. By examining the intensity image, which contained no polarization information, we found that polarization added greatly to the information on surface features, such as details on an entire river system or details on topography that were not clear in the intensity (unpolarized) images.

Combinations of the polarization images were used as input to a principal component analysis, which provided some useful pictorial information not contained in any of the input images. Further benefit was obtained by performing histogram equalization on the principal component images prior to applying the inverse transformation, thus decorrelating the input images. This technique provided better definition of features not observed in the unpolarized sum image. However, such approaches are empirical and cannot, at this time, be employed in a deterministic fashion.

By differencing the Fourier spectra of the polarization image pair, we found that significant differences exist between the images in the population, azimuthal distribution and spatial frequency distribution of contrast boundaries. If contrast across a boundary is reduced, then there will be a point at which the contrast difference will cease to be observed, since it will disappear into the noise. Conversely, appropriate use of polarization methods may render contrast boundaries more readily observable by increasing contrast differences across the boundary, thus reducing clutter and improving signal-to-noise ratio, as observed by Coulson, Whitehead, and Campbell.[10] In fact, for the image of the El Richat structure we found that topographic details were considerably enhanced by digitally manipulating the polarization image pairs.

6. ACKNOWLEDGMENTS

We acknowledge the help and cooperation of colleagues at our respective institutions. The first author wishes to thank the Naval Ocean Research and Development Activity for their generosity in making their facilities available for image analysis and for manuscript preparation. A portion of the work was funded by the NASA/JSC Directors Discretionary Fund. We thank Becky Rotundo for her careful preparation of the draft manuscript and Linda Jenkins for editorial work.

7. REFERENCES

1. Egan, W., "Optical Stokes parameters for farm crop identification," *Remote Sensing of Environment*, Vol 1, pp. 165-180, 1970.

2. Vanderbilt, V. C., L. Grant, and C. S. T. Daughtry, "Polarization of light scattered by vegetation," *Proceedings of IEEE*, vol. 73, pp. 1012-1024, 1985.

3. Egan, W., *Photometry and Polarization in Remote Sensing*, Elsevier, New York, 1985.

4. Slater, P. N., "Photographic systems for remote sensing," in *Manual of Remote Sensing* 2nd edition, ed. R. N. Colwell, American Society for Photogrammetry, Falls Church, Virginia, 1983, pp. 231-289, especially pp. 247-248.

5. Talmadge, D. A. and P. J. Curran, "Remote sensing using polarized light," *Internat. J. of Remote Sensing*, vol. 7, pp. 47-64, 1986.

6. Coulson, K. L., "Effects of reflection properties of natural surfaces in aerial reconnaissance," *Appl. Optics*, vol. 5, pp. 905-917, 1966.

7. Coulson, K. L., G. M. Bouricius, and E. L. Gray, "Optical reflection properties of natural surfaces," *J. Geophys. Res.*, vol. 70, pp. 4601-4611, 1965.

8. Halajian, J. and H. Hallock, "Principles and techniques of polarimetric mapping," *Proc. of the Eighth International Symposium on Remote Sensing of Environment*, Ann Arbor, Michigan, p. 523, 1972.

9. Curran, P. J., "A photographic method for the recording of polarized visible light for soil surface moisture indications," *Remote Sensing of Environment*, vol. 7, pp. 305-322, 1978.

10. Coulson, K. L., V. S. Whitehead, and C. Campbell, "Polarized views of the earth from orbital altitude," *SPIE*, vol. 637; *Ocean Optics VIII*, pp. 35-41, 1986.

11. Coulson, K. L., *Polarization and Intensity of Light in the Atmosphere*, A. Deepak Publishing, Hampton, Virginia, 1988.

12. Hecht, E., *Optics*, second ed., Addison-Wesley, Reading, Mass, 1987.

13. Chandrasekhar, S., *Radiative Transfer*, Dover, New York, 1960.

14. Spohr, G. U., Messung der polarisation von streulicht uber wasserflachen, Ph.D., Thesis, Koln, 1978.

15. Prosch, T., D. Hennings, and E. Raschke, "Video polarimetry: a new imaging technique in atmospheric science," *Appl. Optics*, vol. 22, pp. 1360-1363, 1983.

16. Walraven, R., "Polarization imagery," *Optical Engng.*, vol. 20, pp. 15-18, 1981.

17. Coulson, K. L., "Effect of surface reflection on the angular and spectral distribution of skylight," *J. Atmospheric Sciences*, vol. 25, pp. 759-770, 1968.

18. Duggin, M. J., "Factors limiting the discrimination and quantification of terrestrial features using remotely sensed radiance," *Internat. J. Remote Sensing*, vol. 6, pp. 3-27, 1985.

19. Rao, C. R. N., "Balloon measurements of the polarization of light diffusely reflected by the earth's atmosphere," *Planet. Space Sci.*, vol. 17, pp. 1307-1309, 1969.

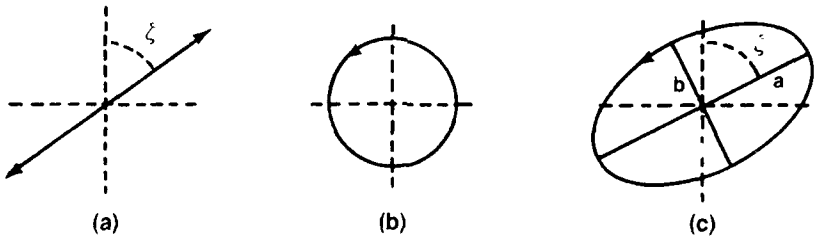

Fig. 1. The three states of polarization. Here, the mean electric vector of recorded radiance is viewed along the direction of propagation.[5] *(a) Shows a state of linear polarization, where the mean electric vector does not rotate about the direction of propagation with time. (b) Shows a state of circular polarization in which the ensemble of propagated electromagnetic waves produces the same effect as two orthogonal waves which are out of phase. The amplitude is constant, but the electric vector rotates with time about the direction or propagation. (c) Shows the elliptical polarization case where the amplitude of the resultant wave varies with time as its plane rotates about the direction of propagation. Here, ζ is the orientation of the polarization ellipse with respect to a reference direction.*

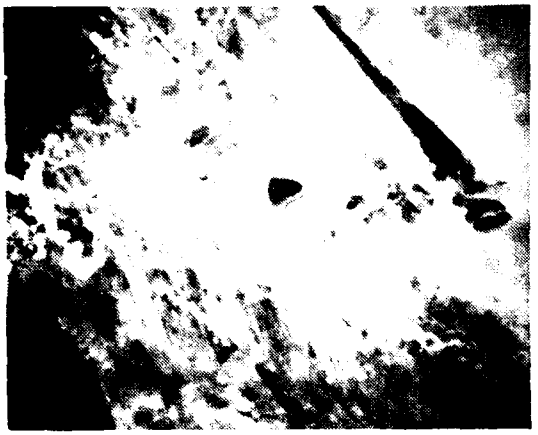

Fig. 2(a). Maximum intensity image (A) of the Niger River.

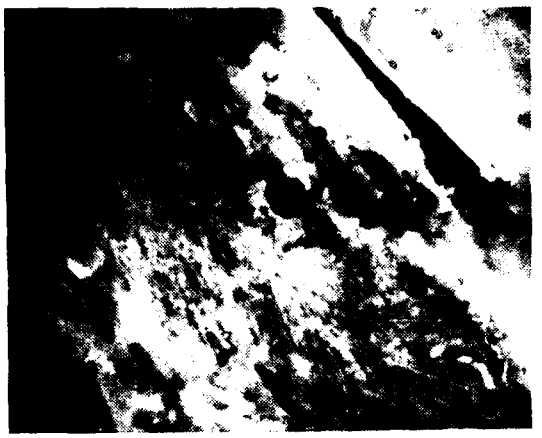

Fig. 2(b). Minimum intensity image (B) of the Niger River.

Fig. 2(c). Difference image (A–B).

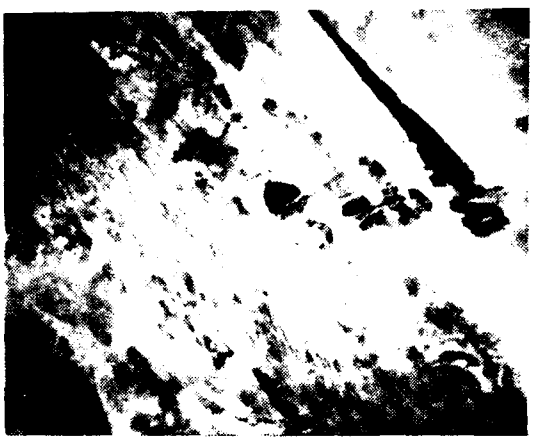

Fig. 2(d). Sum image (A + B).

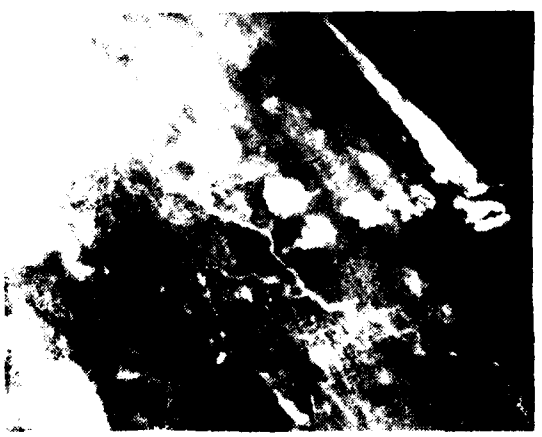

Fig. 2(e). Degree of polarization image (A–B)/(A + B).

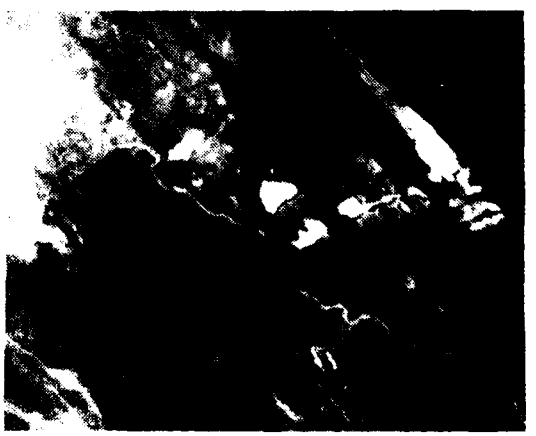

Fig. 2(f). Ratio image (A/B).

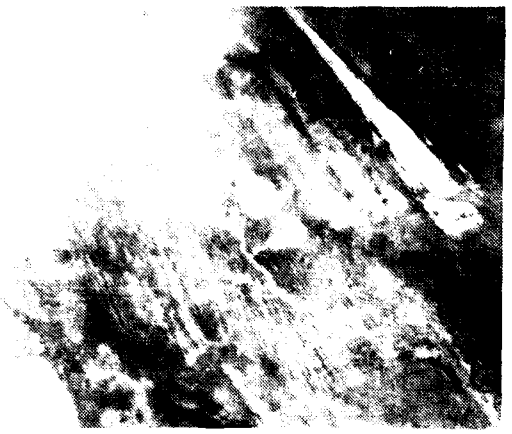

Fig. 2(g). First principal component image.

Fig. 2(h). Second principal component image, which shows more detail of the Niger River than image A.

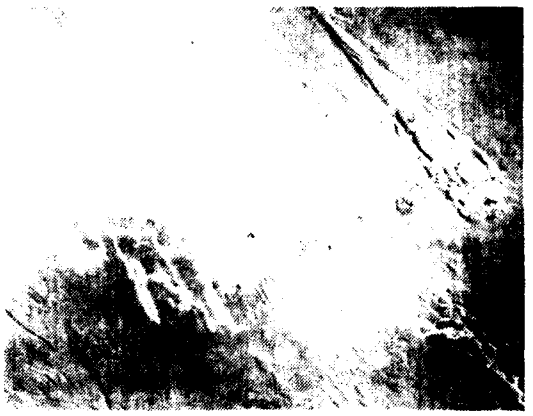

Fig. 2(i). First inverse principal component image after histogram equalization of the principal component images and application of the inverse transformation matrix.

Fig. 2(j). Maximum and minimum intensity images constituting the polarization pair of the Niger River, together with the difference of their power spectra.

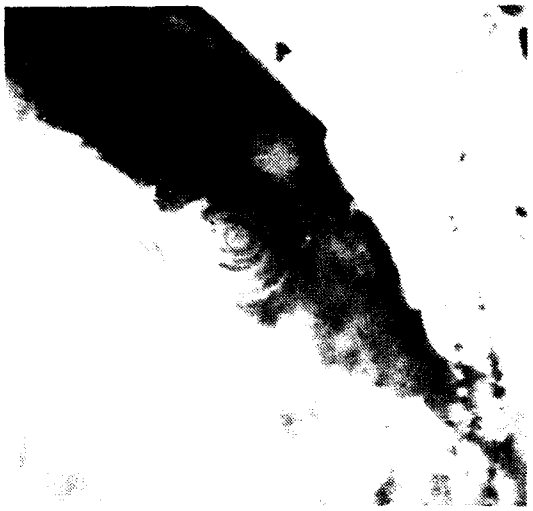

Fig. 3(a). Maximum intensity image (A) of the El Richat structure.

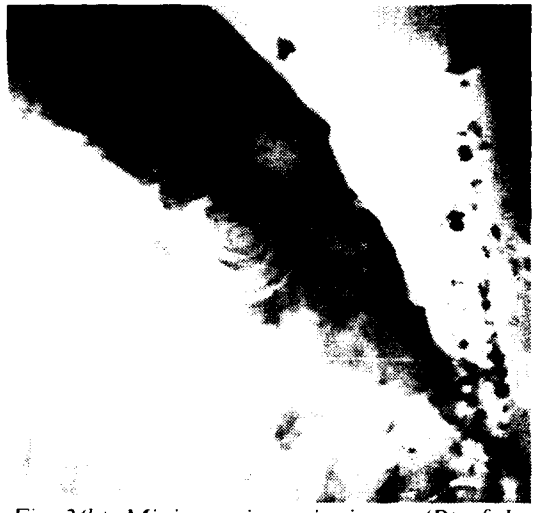

Fig. 3(b). Minimum intensity image (B) of the El Richat structure.

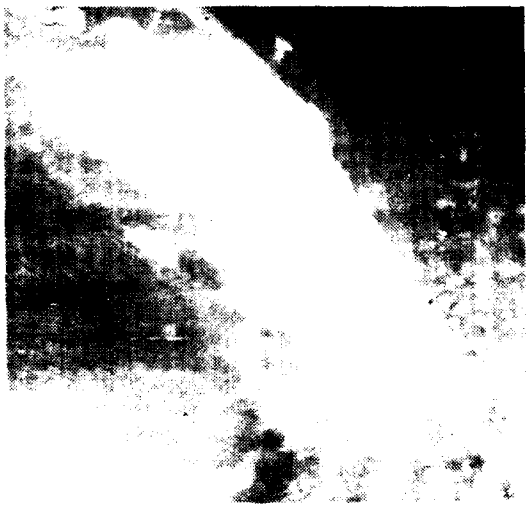

Fig. 3(c). Difference image (A–B).

Fig. 3(d). Degree of polarization image (A–B)/(A + B).

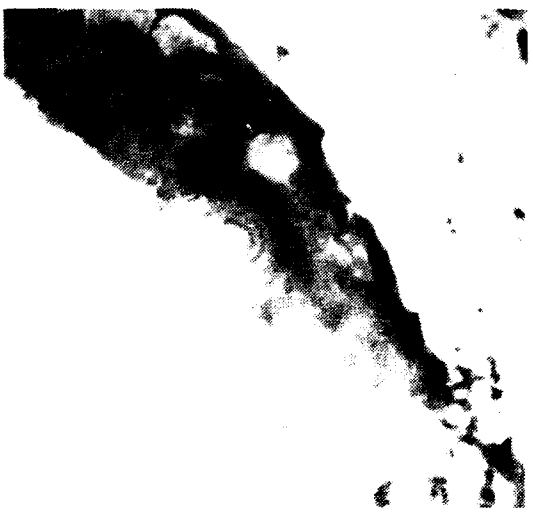

Fig. 3(e). Sum image (A + B).

Fig. 3(f). Ratio image (A/B).